Conformation of Ring Polymers in 2D Constrained Environments

G. Witz, K. Rechendorff, J. Adamcik, and G. Dietler

Laboratoire de Physique de la Matière Vivante, Ecole Polytechnique Fédérale de Lausanne (EPFL), CH-1015 Lausanne, Switzerland

(Received 11 December 2010; published 15 June 2011)

The combination of ring closure and spatial constraints has a fundamental effect on the statistics of semiflexible polymers such as DNA. However, studies of the interplay between circularity and constraints are scarce and single-molecule experimental data concerning polymer conformations are missing. By means of atomic force microscopy we probe the conformation of circular DNA molecules in two dimensions and in the concentrated regime (above the overlap concentration c^*). Molecules in this regime experience a collapse, and their statistical properties agree very well with those of simulated vesicles under pressure. Some circular molecules also create confining regions in which other molecules are trapped. Thus we show further that spatially confined molecules fold into specific conformations close to those found for linear chains, and strongly dependent on the size of the confining box.

DOI: 10.1103/PhysRevLett.106.248301 PACS numbers: 82.35.Gh, 87.64.Dz, 36.20.Ey, 87.14.gk

Ring closure of a polymer is one of the important factors influencing its statistical mechanical properties [1], e.g., scaling [2,3], shape [4,5], and diffusion [6–8], because it restrains the accessible phase space. The theoretical description of circular chains (knots or catenanes) is a challenging problem, owing to the difficulties inherent to a systematic theoretical analysis of such objects constrained to a unique topology. The problem is particularly evident for systems of interacting chains, for example, in semidilute or confined states. Cates and Deutsch [9] pointed out that topological constraints act to alter quite dramatically the behavior of chains in a melt. This has been confirmed by experiments and simulations for the three-dimensional (3D) system [10], but to our knowledge not for the 2D case where studies are limited to the linear case [11].

The behavior of confined circular chains remains also poorly understood, and only a few experiments explored this system [12]. Ring closure, and more generally topology, plays a key role in a wide range of biophysical contexts where DNA is constrained: segregation of the compacted circular genome of some bacteria [13], formation of chromosomal territories [14] in cell nuclei, compaction and ejection of the knotted DNA of a virus [15,16], migration of a circular DNA in an electrophoresis gel [17] or in a nanodevice such as a nanochannel [18], or localization of knots [3,19]. Therefore a better understanding of the basic properties of such systems is highly needed.

In the present Letter, we would like to present experimental findings on ring polymers in the concentrated phase and in a confined environment obtained at the single-molecule level by means of the atomic force microscope (AFM) as depicted in Fig. 1.

A 10 μl drop of nicked circular-plasmid DNA pBR322 (4361 base pairs) at a concentration of 0.5 mg/ml in 1 mM $MgCl_2$ was deposited for 5 minutes on a freshly cleaved mica surface, then rinsed with 10 ml of ultrapure water and dried. The samples were then imaged in tapping mode with silicon nitride probes on a Nanoscope III Veeco AFM. These samples offered us the possibility to study both the semidilute state and the confined state. Indeed, the majority of molecules in these samples are collapsed in the semidilute phase [e.g., Fig. 2(a); the collapse is evidenced in the measure of the area enclosed by the molecules—see Table I], but in addition, some molecules can be trapped inside the perimeter of another already present on the surface, leading to a rearrangement of both molecules [e.g., Fig. 2(c)]: the outer one experiences swelling (also evidenced through area measurement, see Table I) and the inner one is confined within an approximately circular boundary. For clarity, we separate the different molecular states into 3 classes: class I refers to those molecules in dense overlapping phase [the semidilute regime, $c > c^*$, shown in Fig. 2(a)]; class II refers to swollen molecules [Fig. 2(c)]; class III covers confined molecules (Fig. 3). Additionally, we systematically compare these three classes to the dilute case, analyzed in previous publications [20–22]. Nicking ensures that no confounding supercoils are present, and the deposition technique ensures that the molecules equilibrate in two dimensions [20], meaning

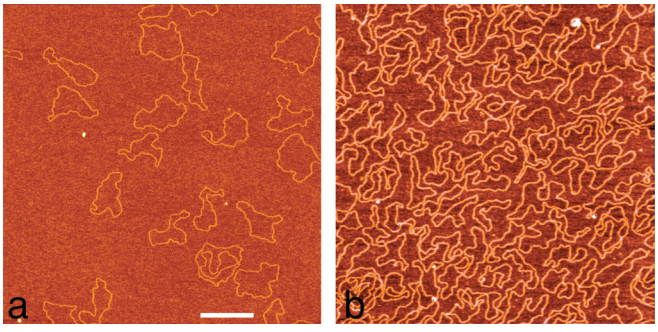

FIG. 1 (color). Nicked pBR322 plasmids deposited at (a) low and (b) high density on mica (the white scale bar represents 500 nm).

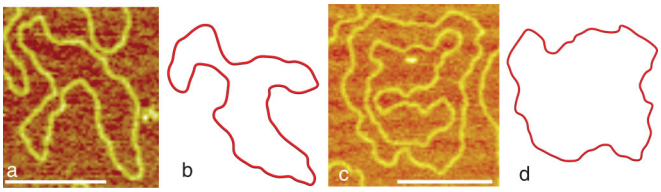

FIG. 2 (color). Representative images of (a) a DNA molecule collapsed in the semidilute phase (class I), (b) a simulated chain with $\Delta p < 0$, (c) a swollen DNA chain (class II), and (d) a simulated chain with $\Delta p > 0$ (white scale bars are 250 nm).

that most of the intra- and interchain crossings are suppressed. To ensure good comparison with theory, the few molecules presenting chain crossings are discarded before the analysis.

From the AFM images, the trajectories of individual molecules were determined [23] separately for each class, and used to calculate the different statistical quantities needed to test both theoretical and numerical predictions. In particular, we wanted to verify whether collapsed (class I) and swollen (class II) molecules, exposed to the pressure generated by the excluded volume of surrounding or enclosed chains, could be treated as 2D vesicles subject to a homogenous pressure. To this end, we simulated pressurized 2D vesicles following the model originally proposed by Leibler, Singh, and Fisher (the LSF model) [24]. These vesicles are 2D self-avoiding boundaries with a difference of pressure between their geometrical in- and outside. For the simulation, the vesicle boundary is partitioned into N cylindrical segments whose vertices are randomly displaced following a Monte Carlo Metropolis algorithm. The energy function of the Metropolis criteria is composed of potentials reproducing the physical properties of the pBR322 molecules: the length is conserved by giving an infinite energy to segments deviating by more than $\pm 25\%$ from their original length, the bending energy is given by the bending potential $E_b = g\Sigma_{i=1}^{N}\theta_i^2$ where θ_i is the deflection angle between segments i and $i+1$, and g the bending constant setting the persistence length to $l_p = 50$ nm. Self-avoidance is respected by giving a radius of 3 nm to each segment and by setting the energy of self-intersecting conformations to infinity. Finally, as in Leibler, Singh, and Fisher [24], to simulate the pressure difference a term proportional to the molecule area S is added, $E_p = \Delta p S$. Figures 2(b) and 2(d) show snapshots

TABLE I. Shape parameters and area (in units of the dilute circular molecules).

Class	Area	Σ	A
I semidilute	0.73	0.272 ± 0.02	0.4 ± 0.02
II swollen	1.66	0.6 ± 0.01	0.082 ± 0.006
III confined	0.57	0.42 ± 0.03	0.2 ± 0.02
Dilute	1.0	0.38 ± 0.02	0.27 ± 0.02

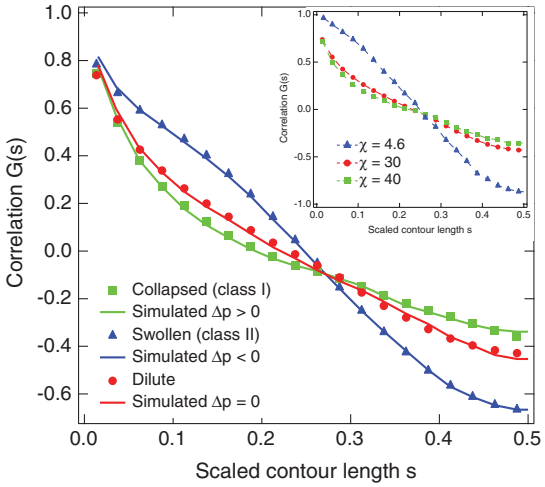

FIG. 3 (color). Bond correlation functions $G(s)$ for circular DNA under different conditions (points) and for simulated molecules under different pressures Δp (full lines). The inset shows $G(s)$ for DNA molecules of different rigidities χ in the dilute case.

of such vesicles with negative and positive pressures, respectively.

Visual comparison of imaged and simulated molecules in Fig. 2 already suggests a good correspondence between data and model. We now verify this by measuring statistical polymer properties, and begin by treating the bond correlation functions $G(s)$ of chains in semidilute phase (class I molecules) and of swollen chains (class II molecules) together because of their similarity. The function $G(s)$ gives the orientational correlation along the chain between two points separated by a contour length s. In the ideal case of a linear Gaussian chain, the correlation function decays exponentially, $G(s) = \exp(-s/l_p)$, with a characteristic persistence length l_p. However, more complex effects, such as self-avoidance, specific topologies, or a high polymer concentration, are reflected in different shapes for $G(s)$, which expresses these constraints in a compact form [22,25,26]. The bond correlation functions are presented in Fig. 3, and compared to the dilute case. Molecules in the overlapping phase are characterized by a more rapid initial decay of $G(s)$ followed by a weaker anticorrelation. For swollen chains, exactly the opposite behavior is observed, namely, a slower initial decay followed by a stronger anticorrelation. This agrees with visual observation of the molecules in Fig. 2, where swollen chains appear to be stiffer than chains in the dilute phase, whereas the opposite applies for chains in the overlapping phase.

In Fig. 3, the experimentally measured correlation functions are compared to those extracted from the numerical simulations of vesicles under pressure. The behavior of both swollen and collapsed chains can be recovered by tuning Δp, which is positive for collapsed chains and

negative for swollen ones. The Δp values used in Fig. 3 were not extracted from a fit, but were selected from an ensemble of curves as those giving the best match to the data. The agreement between experiments and simulations is excellent, in particular, where the numerical data recover fine details, like, for example, the initial negative curvature of the class II correlation function. This indicates that, at least for $G(s)$, pressurized vesicles and class I and II chains can be described formally by the same theory. This simplification of the problem may be extended still further: comparing the ensemble of curves in Fig. 3 with that corresponding to chains of different rigidities $\chi = L/l_p$ (L is the total length of the chain), reproduced from Ref. [20] as the inset in Fig. 3, it is clear that the above mentioned intuitive relation between rigidity and pressure is correct. Thus a polymer ring in the semidilute regime may be viewed, when considering only the bond correlation function, simply as a ring with variable rigidity.

From our results for the correlation function, ring polymers in classes I and II are clearly described very well by the LSF model, and thus we pursue our comparison with the results of Fisher and coworkers who extensively studied the shape parameters of vesicles. As the correlation function, these shape parameters are convenient measures characterizing the different polymer classes because they depend on the type of polymer (Gaussian, self-avoiding), its dimensionality, its topology, and its rigidity [4,5,27,28]. Typical shape measures include the anisotropy Σ and the asphericity A, which are defined as combinations of R_{G1}^2 and R_{G2}^2, the small and large principal axes of the radius-of-gyration tensor R_G, by $\Sigma = \langle R_{G1}^2/R_{G2}^2 \rangle$ and $A = \langle (R_{G1}^2 - R_{G2}^2)^2/(R_{G1}^2 + R_{G2}^2)^2 \rangle$.

Using these shape parameters, Camacho and Fisher [28] have investigated the different phases of vesicles as functions of Δp and χ. In particular, they showed that vesicles with moderate χ changed their behavior from self-avoiding walk to lattice animal by increasing Δp from 0 to large positive values. Indeed upon increasing Δp, vesicles fold on themselves, and create branched structures made of loops, which belong to the same universality class as lattice animals. Here we investigate whether the DNA rings compressed in the semidilute phase also fold in this particular way, as it has been shown theoretically in 3D [29]. At $\Delta p = 0$, the molecules are simply considered as self-avoiding chains, for which Σ was estimated numerically by Bishop and Saltiel [27] to be $\Sigma = 0.4$, and recalculated in Ref. [28] as $\Sigma = 0.39$. Our experimental result for measurements in the dilute case is $\Sigma = 0.38 \pm 0.02$, in very good agreement with the latter values. The anisotropy for lattice animals was calculated by Family, Vicsek, and Meakin. [30] to be $\Sigma_\infty = 0.29$, and in the LSF model [28] to be $\Sigma = 0.275$. Our results for class I molecules, which do experience a folding, yield $\Sigma = 0.272 \pm 0.02$, a value in very good agreement with the numerical estimates for both lattice animals and compressed vesicles. The values are summarized in Table I, where asphericity values are provided as well as supplementary information. The agreement of our estimates with the numerical values, combined with the above analysis of $G(s)$, strongly supports the analogy between circular polymers in the semidilute phase and vesicles under pressure. We note in passing that a similar shape analysis for swollen chains (class II molecules) is of no interest, because the anisotropy simply tends towards $\Sigma = 1$. We are able only to confirm that the anisotropy of swollen chains is indeed larger than in the dilute case (Table I).

We now turn our attention to the confined chains (class III) depicted in Fig. 4. We stress that it is very difficult to design an experiment allowing one to probe the local conformation of confined, semiflexible polymers from the nanometer scale to the micron scale. In the present case, it is the swollen chains which create the confining geometry, a nearly circular box of contour length s equal to that of pBR322 DNA. Consequences of confinement are clearly visible in the oscillatory behavior of the correlation function $G(s)$, as visible in Fig. 4. This feature has been observed numerically in 3D for semiflexible linear and ring strings confined within spheres, where the chains experience a buckling in the form of a saddle [31,32], as well as for the semiconfinement of a linear chain in a tube [18], and yet more obviously for 2D linear chains confined in circular and rectangular boxes [33]. In the last study, the authors explored the interplay between the box size W and the chain rigidity l_p by analyzing $G(s)$. In explaining the oscillatory behavior of $G(s)$, they found that once $l_p \simeq W$, linear chains fold into specific conformations to limit the bending-energy penalty: either stable and spiral-like or unstable double-folded conformations. Interestingly, the latter conformation is also adopted by the imaged circular

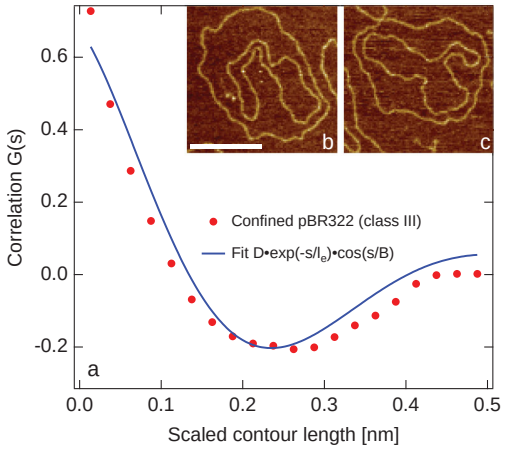

FIG. 4 (color). (a) The bond correlation function $G(s)$ for confined DNA molecules (class III) is compared to the analytical approximation proposed by Liu and Chakraborty [33]. (b) and (c) Examples of confined conformations (class III). Conformations of type (b), a curved double-fold, represent the majority of cases (the white scale bar is 250 nm).

DNA chains, showing that under space constraint, ring and linear molecules behave similarly. This is supported by analyzing the data with the help of the approximate correlation function provided by the same authors for confined linear chains $G(s) = D\exp(-s/l_e)\cos(s/B)$, where D is a numerical factor, B a length scale related to W, and l_e an effective persistence length. The fit to our data using that equation is shown in Fig. 4. At the qualitative level, the agreement is excellent; quantitatively, the deduced value $B \simeq 127$ nm corresponds closely to half the radius of a perfectly circular pBR322 chain, $R = 238$ nm. This matches very well the findings of Liu and Chakraborty [33] that in general $B = W/2$. The value of the effective persistence length is $l_e = 307$ nm, showing that the constraint of confinement maintains the molecules in rather rigid conformations. Our results therefore demonstrate that the effects of confinement are extremely strong, forcing the molecules to adopt a very limited set of configurations. Further, this set of configurations is to a certain extent shared between ring and linear molecules.

By analyzing AFM images of semidilute samples of circular DNA, we have performed the first experimental investigation of polymeric systems which have to date received intensive but exclusively theoretical attention. Our direct measurements of shape parameters and correlation functions demonstrate a number of fundamental properties of polymers. In particular, we have shown that the vesicle model of Leibler, Singh, and Fisher [24] is very effective in describing the semidilute phase of circular polymers. The utility of this link between the two problems cannot be underestimated, because it has also been shown [34] that circular polymers confined in an array of obstacles and folding into lattice-animal conformations can be mapped to the problem of vesicles under pressure. Thus three apparently disconnected problems exhibit very similar types of behavior, greatly simplifying their understanding due to the range of different theoretical and numerical tools which may be used to explain them. Our data also demonstrate that circular DNA can be efficiently used as a nanowell to study polymer confinement down to the nanometer level.

We thank Andrzej Stasiak and Ralf Metzler for their valuable comments. This investigation was supported by the Swiss NSF through Grants No. 200021-116515 and No. 200020-125159. K. R. is grateful to the Carlsberg and Novartis Foundations for financial support.

[1] J. Des Cloizeaux, J. Phys. Lett. **42**, L433 (1981).
[2] A. Dobay *et al.*, Proc. Natl. Acad. Sci. U.S.A. **100**, 5611 (2003).
[3] E. Ercolini *et al.*, Phys. Rev. Lett. **98**, 058102 (2007).
[4] K. Alim and E. Frey, Phys. Rev. Lett. **99**, 198102 (2007).
[5] E. J. Rawdon *et al.*, Macromolecules **41**, 8281 (2008).
[6] S. Araki *et al.*, Chem. Phys. Lett. **418**, 255 (2006).
[7] R. M. Robertson, S. Laib, and D. E. Smith, Proc. Natl. Acad. Sci. U.S.A. **103**, 7310 (2006).
[8] G. Tsolou, N. Stratikis, C. Baig, P. S. Stephanou, and V. G. Mavrantzas, Macromolecules **43**, 10 692 (2010).
[9] M. E. Cates and J. M. Deutsch, J. Phys. (Paris) **47**, 2121 (1986).
[10] T. Vettorel, A. Y. Grosberg, and K. Kremer, Phys. Biol. **6**, 025 013 (2009).
[11] B. Maier and J. O. Rädler, Macromolecules **33**, 7185 (2000); H. Meyer, J. P. Wittmer, T. Kreer, A. Johner, and J. Baschnagel, J. Chem. Phys. **132**, 184 904 (2010).
[12] F. Persson *et al.*, Nano Lett. **9**, 1382 (2009).
[13] S. Jun and B. Mulder, Proc. Natl. Acad. Sci. U.S.A. **103**, 12 388 (2006).
[14] J. Dorier and A. Stasiak, Nucleic Acids Res. **37**, 6316 (2009).
[15] D. Marenduzzo and C. Micheletti, J. Mol. Biol. **330**, 485 (2003).
[16] R. Matthews, A. A. Louis, and J. M. Yeomans, Phys. Rev. Lett. **102**, 088101 (2009).
[17] S. P. Obukhov, M. Rubinstein, and T. Duke, Phys. Rev. Lett. **73**, 1263 (1994).
[18] W. Reisner *et al.*, Phys. Rev. Lett. **94**, 196101 (2005).
[19] A. Hanke *et al.*, Eur. Phys. J. E **12**, 347 (2003); R. Metzler *et al.*, Phys. Rev. Lett. **88**, 188101 (2002).
[20] G. Witz, K. Rechendorff, J. Adamcik, and G. Dietler, Phys. Rev. Lett. **101**, 148103 (2008).
[21] F. Drube *et al.*, Nano Lett. **10**, 1445 (2010).
[22] T. Sakaue, G. Witz, G. Dietler, and H. Wada, Europhys. Lett. **91**, 68 002 (2010).
[23] J. Marek *et al.*, Cytometry Part A **63A**, 87 (2005).
[24] S. Leibler, R. R. P. Singh, and M. E. Fisher, Phys. Rev. Lett. **59**, 1989 (1987).
[25] A. Baumgärtner, J. Chem. Phys. **76**, 4275 (1982).
[26] K. Shimomura, H. Nakanishi, and N. Mitarai, Phys. Rev. E **80**, 051804 (2009).
[27] M. Bishop and C. J. Saltiel, J. Chem. Phys. **85**, 6728 (1986).
[28] C. J. Camacho and M. E. Fisher, Phys. Rev. Lett. **65**, 9 (1990).
[29] S. T. Milner and J. D. Newhall, Phys. Rev. Lett. **105**, 208302 (2010).
[30] F. Family, T. Vicsek, and P. Meakin, Phys. Rev. Lett. **55**, 641 (1985).
[31] A. Maritan, C. Micheletti, A. Trovato, and J. R. Banavar, Nature (London) **406**, 287 (2000).
[32] K. Ostermeir, K. Alim, and E. Frey, Phys. Rev. E **81**, 061802 (2010).
[33] Y. Liu and B. Chakraborty, Phys. Biol. **5**, 026 004 (2008).
[34] D. Gersappe and M. Olvera de la Cruz, Phys. Rev. Lett. **70**, 461 (1993).